

Practical Chromatic Aberration Correction in Virtual Reality Displays Enabled by Cost-Effective Ultra-Broadband Liquid Crystal Polymer Lenses

Tao Zhan, Junyu Zou, Jianghao Xiong, Xiaomin Liu, Hao Chen, Jilin Yang, Sheng Liu, Yajie Dong, and Shin-Tson Wu*

Chromatic aberration (CA) is a critical issue in immersive virtual reality displays. The current digital compensation method can reduce the CA by pre-processing the image contents but at the cost of extra memory space, processing time, and power consumption. Moreover, it is not possible to digitally compensate the CA within each color channel. Here, a practical optical approach is presented to correct the CAs, including the sub-channel ones, in the virtual reality system, whose functionality is verified by both ray-tracing analysis and experimental results. In this device, a compact ultra-broadband Pancharatnam-Berry phase lens (PBL) with complex axial molecular structure is fabricated and then hybridized with a refractive Fresnel lens. Due to their opposite chromatic dispersion, the system's CA is significantly reduced. To eliminate ghost image from the zero-order leakage of PBL, a broadband circular polarizer is implemented to block the stray light. As a result, clear image within the entire 100° field-of-view is achieved. The proposed large-size cost-efficient broadband wide-view flat optics can practically benefit not only virtual reality displays but also general imaging systems for practical applications and scientific research.

been developed in recent years. To offer immersive VR experience, the field of view (FOV)^[1] should be >100° in the viewing optical system,^[2] which results in considerable color break-up around objects, especially at the periphery. This visual artifact is known as chromatic aberration (CA) due to the wavelength-dependent focal length of the viewing optics, as illustrated in Figure 1a, which originates from the dispersive nature of electric permittivity. Although the noticeability of this phenomenon is dependent on the user's gaze point and the displayed image content, it is highly desirable to provide chromatic aberration correction (CAC) for better user experience.

There are mainly two types of CAC method, digital and optical. At the cost of extra graphic computation power, the CA can be significantly reduced by pre-processing images according to the chromatic dispersion of viewing optics, which is a digital compensation method similar to the lens correction in photography.^[3] The digital CAC helps decrease but cannot completely eliminate CA, because each color channel has a spectral bandwidth unless laser displays are implemented. The sub-channel aberrations could be more apparent for panels with higher pixel density. From a systematic perspective, the processing time occupied by digital CAC in each frame would increase as both resolution and frame rate increase in the future VR devices. Also, in portable VR devices, where power consumption is a big concern, the memory- and computation-consuming digital CAC may not be affordable.

Optical CAC has been widely applied as a useful and necessary part in chromatic imaging systems since the 18th century.^[4] Conventional optical CAC approach utilizes two or more lens materials with different refractive index dispersions, or Abbe numbers, in the system to unite the focal length at two or more wavelengths.^[5] However, achromatic doublets are more expensive and heavier than singlets in head-mounted display systems, causing discomfort to the users. In late 1900s, another approach based on the hybrid of diffractive and refractive lenses was developed,^[6] exploiting the negative Abbe number of diffractive elements. Despite their demanding fabrication process, diffractive Fresnel phase lenses have been integrated

Thanks to the rapid development of robust mobile processors, high-pixel-density display panels, and optics fabrication capabilities, decent virtual reality (VR) near-eye display devices have


T. Zhan, J. Zou, J. Xiong, Prof. X. Liu, Dr. H. Chen, Prof. Y. Dong,
Prof. S.-T. Wu

CREOL
The College of Optics and Photonics
University of Central Florida
Orlando, FL 32816, USA
E-mail: swu@creol.ucf.edu

Prof. X. Liu
School of Physics and Engineering
Zhengzhou University
Zhengzhou 450001, China

J. Yang, Dr. S. Liu
GoerTek Electronics
5451 Great America Parkway, Suite 301, Santa Clara, CA 95054, USA

Prof. Y. Dong
Department of Materials Science & Engineering
University of Central Florida
Orlando, FL 32816, USA

 The ORCID identification number(s) for the author(s) of this article can be found under <https://doi.org/10.1002/adom.201901360>.

DOI: 10.1002/adom.201901360

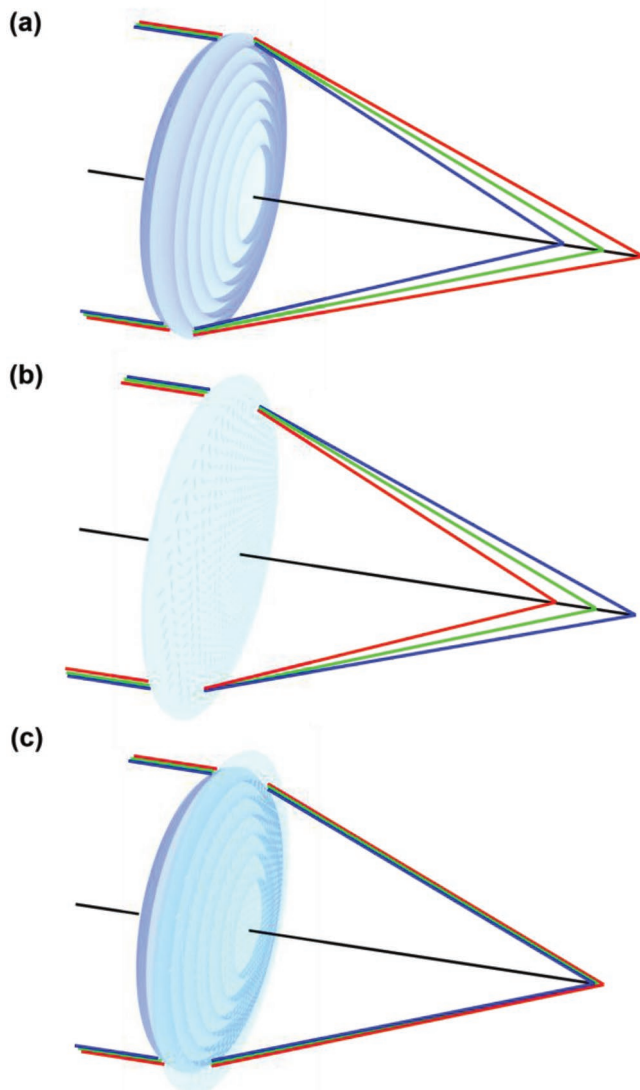


Figure 1. Illustration of a) a compact refractive Fresnel lens showing CAs, b) a diffractive PBL manifesting opposite CAs, and c) the proposed hybrid lens set exhibiting achromatic performance.

into consumer lens systems to pursue compact size and better imaging performance.^[7]

In this paper, we propose to apply low-cost yet high-quality broadband diffractive Pancharatnam-Berry phase lenses (PBLs)^[8–10] to immersive near-eye display systems as a practical CAC element.^[11,12] The PBLs made of liquid crystal (LC) polymer manifest opposite CAs to refractive lenses, as depicted in Figure 1b. Thus, the CAs of VR viewing optics can be effectively reduced if a PBL is attached to the Fresnel surface of the plastic lens, as shown in Figure 1c. Compared to conventional diffractive optical elements and metasurfaces, the fabrication of PBLs is simpler and more cost-effective.^[13–15] Also, PBLs are polarization sensitive, thus the stray light from diffraction leakage can be eliminated by a polarizer. Moreover, PBLs usually have a flat physical geometry with a thickness of only several microns, which can flawlessly satisfy the need for lightweight and compactness in head-mounted displays.

The Pancharatnam-Berry phase optical elements^[16,17] function by a spatial-varying phase change generated through a closed path in the polarization parameter space, which is commonly realized using a patterned LC half-wave plate. The orientation of LC molecules at each spatial point on the lens surface determines the local phase change, which is similar to the orientation of the unit element in conventional metasurfaces. Despite the spin-orbit interaction of light embedded in this effect, it can be conveniently represented by Jones calculus with a circularly polarized input light

$$\begin{bmatrix} \cos 2\varphi & \sin 2\varphi \\ \sin 2\varphi & -\cos 2\varphi \end{bmatrix} \begin{bmatrix} 1 \\ \pm i \end{bmatrix} = \begin{bmatrix} 1 \\ \mp i \end{bmatrix} e^{\pm 2i\varphi} \quad (1)$$

where φ denotes the fast axis orientation angle of the half-wave plate or the local LC director. A phase change of 2φ occurs while the handedness of circular polarization is inverted. Thus, PBLs can be fabricated by patterning LC molecular orientation, i.e., φ , in a paraboloidal manner in the radial direction. Thanks to its continuous phase profile and flat geometry, PBLs provide higher optical quality and less stray light in comparison with Fresnel phase lenses. It should be noticed that PBLs manifest opposite optical power for the right-handed and left-handed circularly polarized lights, as Equation (1) indicates. Thus, a broadband quarter-wave ($\lambda/4$) plate should be employed to convert the linearly polarized light from the liquid crystal display panel to circularly polarized light when PBLs are utilized for CAC, as Figure 2a depicts.

For display panels that emit unpolarized light, such as light-emitting diodes, the $\lambda/4$ plate could be replaced by a circular polarizer. Although the high-efficiency bandwidth of PBL may be enhanced with multiple axial layers, it is still quite challenging to achieve large spectral and angular bandwidth simultaneously. Thus, ghost images caused by the zero-order diffraction should be expected especially at the peripheral FOV. To eliminate the zero-order leakage of PBL, a broadband wide-view circular polarizer is placed between the PBL and Fresnel lens such that the undesired ghost image with the other handedness can be removed, as illustrated in Figure 2b. Moreover, based on the optical raytracing analysis of the proposed system, adding a diffractive PBL can improve not only the chromatic color shift but also the general imaging quality of a VR system, as compared in Figure 2c,d.

To make full use of light at visible spectrum from the display panel, ultra-broadband PBLs were fabricated for the proposed system. The procedure is similar to that of conventional PBLs, as described in our previous work,^[14] but here a more complicated sandwich-like axial structure, as depicted in Figure 2e, is used to further widen the spectral bandwidth as mentioned by Zhan et al. and Komanduri et al.^[17,18] Different from conventional metasurface, the PBLs manifest ideally flat geometry even in nanoscale and the LC molecules inside employ a complex structure, right-hand twist, nontwist, and left-hand twist from one substrate to the other. With more degrees of freedom, the bandwidth of the three-layer system is designed to be wider than that of the two-layer structure.^[19,20] As a result, it is able to cover most of the light from display panel, especially at the blue and red edges of visible spectrum.

During device fabrication, first, a photo-alignment layer was created on a glass substrate by spin-coating a 0.2% solution

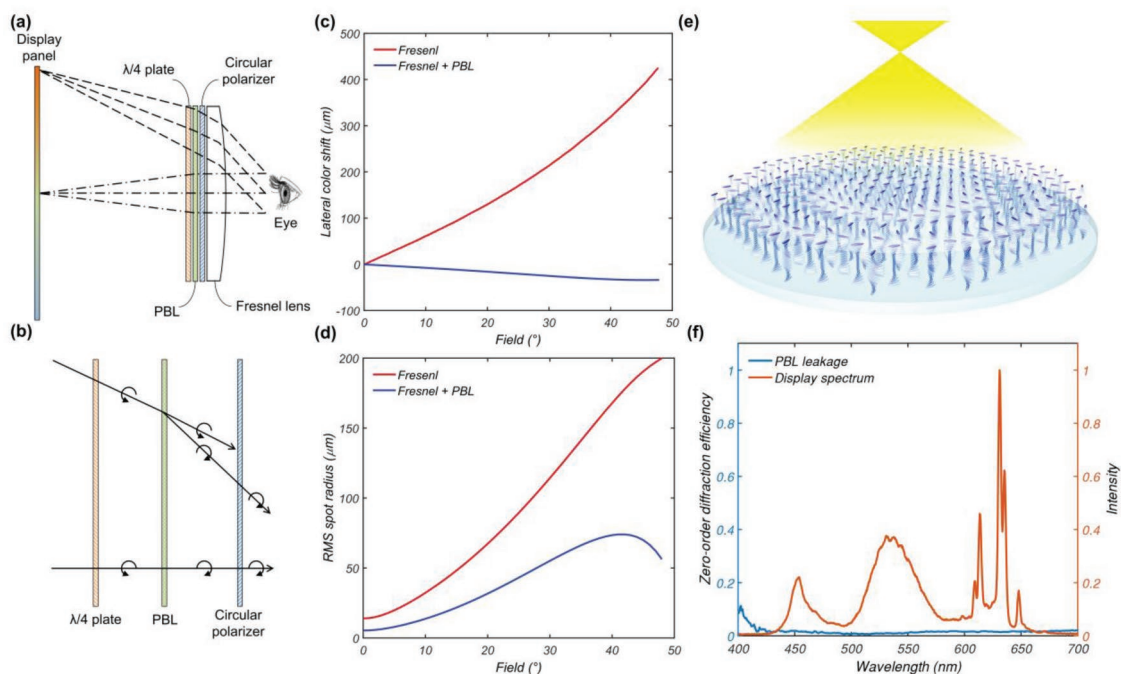


Figure 2. a) Experimental setup of virtual reality display system. b) Schematic illustration of polarization handedness changes through the planar optical parts. Sequential raytracing analysis: c) Lateral color shift and d) RMS spot radius with and without PBL. e) Schematic illustration of LC anisotropy axis orientation in the PBL with a flat geometry and a twist-homo-twist structure. f) Measured zero-order leakage through chromatic and the ultra-broadband PBL and the spectrum of the LCD displaying white light.

of Brilliant Yellow (BY, TCI America) in dimethylformamide (DMF) solvent. The desired lens profile with a 2 in. diameter and 60 cm focal length at $\lambda = 532$ nm was recorded on the BY layer using polarization holography method^[21] to control the local orientation of LC molecules. After the polarization holographic exposure, we spin-coated four LC reactive mesogen (RM) layers one-by-one to achieve the desired achromatically high first-order diffraction efficiency over most of visible spectrum. Each RM layer was crosslinked with 365 nm UV light for a dosage of ≈ 10 J cm⁻² after spin-coating to form a solid surface, which in turn provides the surface alignment for the

next layer. The detailed recipe of material and spin-coating is summarized in **Table 1**.

The spectrum of zero-order leakage from the fabricated PBL (with sandwich-like axial structure) is measured and results are plotted in Figure 2f. The PBLs were placed between two circular polarizers when the zero-order light leakage spectrum was measured by a spectrometer. The ultra-broadband PBL shows minimal zero-order transmission in a wide spectral range, from 425 to 700 nm, which is enough for the proposed application. Afterward, the PBL was placed between a $\lambda/4$ plate and a circular polarizer and then attached to the Fresnel surface of a 2 in. plastic Fresnel lens with 37 mm focal length for a compact form factor, as illustrated in Figure 2a. Finally, regarding the graphic generation unit, a 6.1 in. in-plane-switching liquid crystal display (LCD) panel with a 1792-by-828 resolution (326 pixels in.⁻¹) was assembled with the optical lens module to form a VR breadboard. Although the LCD has a wide visible spectrum from 400 to 700 nm, most of the visible light can be utilized by the ultra-broadband PBL, as Figure 2f shows. **Figure 3a** shows a photograph of the fabricated ultra-broadband PBL captured in front of the CREOL building. The unpolarized CREOL signage is clearly imaged to two depths due to the polarization-dependent optical power of PBL. And the zero-order diffraction leakage is almost negligible.

Table 1. Recipe of the materials and spin-coating in the PBL fabrication (by weight).

Solution	Solute	Solvent	Solute:Solvent	Coating speed
BY layer	Brilliant Yellow	DMF	$\approx 1:500$	500 (5 s) + 3000 (30 s)
1st RM layer	RM257 (95.05%) Irgacure 651 (2.34%) Zonyl 8857A (0.95%) R811 (1.66%)	Toluene	$\approx 1:3.81$	1900 (90 s)
2nd RM layer	RM257 (97.11%) Irgacure 651 (1.92%) Zonyl 8857A (0.97%)	Toluene	$\approx 1:3.89$	1000 (90 s)
3rd RM layer				850 (90 s)
4th RM layer	RM257 (95.48%) Irgacure 651 (1.93%) Zonyl 8857A (0.927%) S811 (1.66%)	Toluene	$\approx 1:3.83$	950 (90 s)

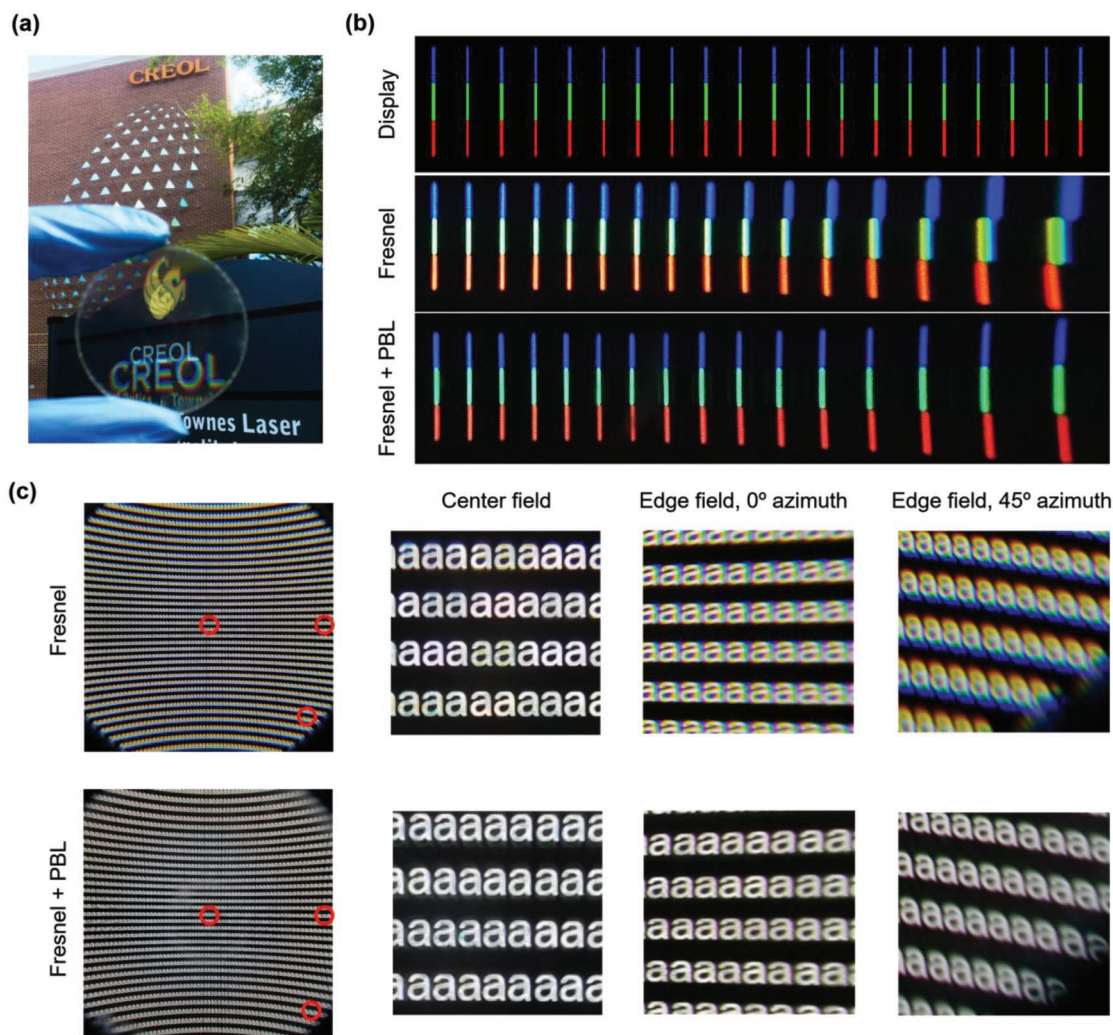


Figure 3. a) Photograph of a fabricated ultra-broadband 2 in. PBL sample. The text “CREOL” is imaged to two depths by the PBL due to its polarization-dependent optical power. b) Half-field CA testing pattern displayed on the LCD and the resulting images captured through the conventional and proposed viewing optics. c) Full-field black and white image displayed on the LCD and the resulting images $\approx 100^\circ$ captured through the conventional and proposed hybrid viewing optics. The three enlarged parts are center field and edge fields at 0° and 45° azimuth from left to right.

To experimentally verify the CAC performance of the proposed system, an image was directly displayed on the LCD screen without barrel distortion correction, which shows a set of evenly spaced bars with RGB segments, as shown in Figure 3b. When viewing through the plastic Fresnel singlet, the test pattern bars are blurred and the RGB colors are apparently displaced due to the transverse CA at peripheral FOV. When the proposed planar optics module, including a PBL sandwiched by a $\lambda/4$ plate and a circular polarizer, is attached to the Fresnel singlet, the color breakup at the edge of FOV is significantly reduced. Figure 3c shows another testing result using a black-and-white image. With the proposed optical structure, the CA can be efficiently corrected at the cost of three planar optical elements without affecting the compact form factor of the system. Although the diffraction efficiency has small difference over the display spectrum, the color variation is not very apparent in the experimental

results. For those applications demanding an ultra-high color accuracy, the image content can be slightly tuned to pre-compensate the small color variation. Furthermore, the proposed cost-effective flat lens can be applied to other imaging and display systems,^[22,23] such as augmented reality^[24,25] and 3D displays,^[26–28] where the CA control is as critical as in virtual reality.

In conclusion, we have designed and demonstrated a prototype VR display system with significantly reduced CAs using planar diffractive optics. We fabricated a key optical element, an ultra-broadband planar polymer lens employing Pancharatnam-Berry phase, manifesting high diffraction efficiency ($>95\%$) over most of the visible spectrum. And due to the low-cost manufacturing of the planar polymer lenses and convenient additive adaptation from current VR devices, the proposed method and system should find widespread applications in the near-eye display industry.

Experimental Section

Material Preparation: The employed LC reactive mesogen was RM257 (LC Matter), whose physical properties are listed as follows: clearing point (T_{NI}) = 108.5 °C, and refractive indices $n_e = 1.69$, $n_o = 1.51$ at $\lambda = 589$ nm. The chiral dopants were S811 and R811 (HCCH, helical twisting power HTP $\approx 12 \mu\text{m}^{-1}$) and the photo-initiator Irgacure 651 (Ciba) was used for LC polymerization. Moreover, the surfactant Zonyl 8857A from DuPont, was also added to achieve a relatively flat air-polymer surface. The detailed weight ratios of their concentration in the precursor are listed in Table 1.

Fabrication Procedures: A 2 in. diameter and 0.4 mm thick glass substrate (Corning Gorilla) was cleaned with acetone, isopropyl alcohol, and de-ionized water, followed by drying in nitrogen. Then the photo-alignment layer was spin-coated on the glass substrate and the solvent was evaporated on a hotplate (60 °C, 5 min). A continuous-wave blue laser emitting at $\lambda = 457$ nm (Cobolt Twist, 200 mW) was employed in the polarization holographic exposure, where the exposure dosage was around 10 J cm^{-2} . After photo-alignment, the sample was coated with RM solutions for four times with a total thickness of $\approx 4.5 \mu\text{m}$. After each RM coating, the sample was exposed to a UV lamp ($\lambda \approx 365$ nm) for photo-polymerization.

Optical Measurements: To characterize the light leakage of the ultra-broadband PBL, a white light source (Mikropack DH-2000) and an optical fiber spectrometer (Ocean Optics HR2000CG-UV-NIR) were used to measure the transmission spectra. The PBL sample was sandwiched between two orthogonal circular polarizers (Edmund Optics #88-100 and #88-102) to show the zero-order light leakage.

Acknowledgements

The UCF group is indebted to GoerTek Electronics for financial support, and Yun-Han Lee for helpful discussion.

Conflict of Interest

The authors declare no conflict of interest.

Keywords

chromatic aberration, liquid crystal polymers, metasurfaces, planar lenses, virtual reality

Received: August 8, 2019

Revised: September 15, 2019

Published online:

- [1] B. Wheelwright, Y. Sulai, Y. Geng, S. Choi, B. Wheelwright, Y. Sulai, Y. Geng, S. Luanava, *Proc. SPIE* **2018**, 10676, 1067604.
- [2] Y. Geng, J. Gollier, B. Wheelwright, Y. Sulai, Y. Geng, J. Gollier, B. Wheelwright, F. Peng, B. Lewis, N. Chan, W. Sze, T. Lam, A. Fix, D. Lanman, Y. Fu, A. Sohn, B. Bryars, *Proc. SPIE* **2019**, 10676, 1067606.
- [3] D. C. Brown, *Photogramm. Eng. Remote Sens.* **1966**, 32, 444.
- [4] F. Watson, *Stargazer: the Life and Times of the Telescope*, Allen & Unwin, Australia **2007**.
- [5] B. E. A. Saleh, M. C. Teich, *Fundamentals of Photonics*, Wiley, New York **1991**.
- [6] T. Stone, N. George, *Appl. Opt.* **1988**, 27, 2960.
- [7] H. Ogawa, *U.S. Patent 6,791,754 B2*, **2004**.
- [8] N. V. Tabiryan, S. R. Nersisyan, D. M. Steeves, B. R. Kimball, *Opt. Photonics News* **2010**, 21, 40.
- [9] T. Zhan, Y. H. Lee, S. T. Wu, *Opt. Express* **2018**, 26, 4863.
- [10] T. Zhan, J. Xiong, Y. H. Lee, S. T. Wu, *Opt. Express* **2018**, 26, 35026.
- [11] N. V. Tabirian, D. E. Roberts, D. M. Steeves, B. R. Kimball, *U.S. Patent 20160047955A1*, **2016**.
- [12] D. Roberts, Z. Liao, J. Y. Hwang, S. R. Nersisyan, N. Tabirian, D. M. Steeves, B. R. Kimball, T. J. Bunning, *Proc. SPIE* **2018**, 10735, 107350Q.
- [13] K. Gao, H. H. Cheng, A. K. Bhowmik, P. J. Bos, *Opt. Express* **2015**, 23, 26086.
- [14] T. Zhan, J. Xiong, Y. H. Lee, R. Chen, S. T. Wu, *Opt. Express* **2019**, 27, 2632.
- [15] Y. Li, Y. Liu, S. Li, P. Zhou, T. Zhan, Q. Chen, Y. Su, S. T. Wu, *Opt. Express* **2019**, 27, 9054.
- [16] Y. H. Lee, G. Tan, T. Zhan, Y. Weng, G. Liu, F. Gou, F. Peng, N. V. Tabirian, S. Gauza, S. T. Wu, *Opt. Data Process. Storage* **2017**, 3, 79.
- [17] T. Zhan, Y. H. Lee, G. Tan, J. Xiong, K. Yin, F. Gou, J. Zou, N. Zhang, D. Zhao, J. Yang, S. Liu, S. T. Wu, *J. Opt. Soc. Am. B* **2019**, 36, D52.
- [18] R. K. Komanduri, K. F. Lawler, M. J. Escuti, *Opt. Express* **2013**, 21, 404.
- [19] N. V. Tabirian, S. V. Serak, S. R. Nersisyan, D. E. Roberts, B. Y. Zeldovich, D. M. Steeves, B. R. Kimball, *Opt. Express* **2016**, 24, 7091.
- [20] C. Oh, M. J. Escuti, *Opt. Lett.* **2018**, 33, 2287.
- [21] L. Nikolova, S. Ramanujam, *Polarization Holography*, Cambridge University, Cambridge **2009**.
- [22] S. Lee, H. Hua, *J. Disp. Technol.* **2014**, 11, 845.
- [23] S. A. Cholewiak, G. D. Love, P. P. Srinivasan, R. NG, M. S. Banks, *ACM Trans. Graph.* **2017**, 36, 210.
- [24] R. Azuma, Y. Baillot, R. Behringer, S. Feiber, S. Julier, B. MacIntyre, *IEEE Comput. Graph. Appl.* **2001**, 21, 34.
- [25] D. Cheng, Y. Wang, H. Hua, M. M. Talha, *Appl. Opt.* **2009**, 48, 2655.
- [26] K. Akeley, S. J. Watt, A. R. Girshick, M. S. Banks, *ACM Trans. Graph.* **2004**, 23, 804.
- [27] S. Liu, H. Hua, D. Cheng, *IEEE Trans. Vis. Comput. Graph.* **2010**, 16, 381.
- [28] X. Hu, H. Hua, *Opt. Express* **2014**, 22, 13896.